Solid-State Electronics 75 (2012) 43–47

Contents lists available at SciVerse ScienceDirect

Solid-State Electronics

journal homepage: www.elsevier.com/locate/sse

Hopping and trap controlled conduction in Cr-doped $SrTiO_3$ thin films

Bach Thang Phan [a,b], Taekjib Choi [c], A. Romanenko [a], Jaichan Lee [a,*]

[a] School of Advanced Materials Science and Engineering, Sungkyunkwan University, Suwon 440-746, Republic of Korea
[b] Faculty of Materials Science and Laboratory of Advanced Materials, University of Science, Vietnam National University, HoChiMinh, Viet Nam
[c] Hybrid Materials Research Center and Faculty/Institute of Nanotechnology and Advanced Materials Engineering, Sejong University, Seoul 143-747, Republic of Korea

ARTICLE INFO

Article history:
Received 13 January 2012
Received in revised form 9 May 2012
Accepted 13 May 2012
Available online 14 June 2012

The review of this paper was arranged by Prof. S. Cristoloveanu

Keywords:
$SrTiO_3$ thin films
Resistive switching
Electrical transport
Variable range hopping
Space charge limited conduction

ABSTRACT

This study examined the electrical conduction of Cr-doped $SrTiO_3$ thin films in a metal (Pt)–insulator–metal ($La_{0.5}Sr_{0.5}CoO_3$) structure. Two DC transport mechanisms, variable range hopping and the trap-controlled space-charge-limited current conduction, were found to be responsible for the conduction behavior. Resistance switching mechanism involved the trapping/detrapping of injected carriers at the weakly localized states.

1. Introduction

Recently, transition-metal oxides with a perovskite structures (Cr-doped $SrZrO_3$, Cr-doped $SrTiO_3$) [1–4] and perovskite manganite structure ($Pr_{0.7}Ca_{0.3}MnO_3$, $La_{0.7}Sr_{0.3}MnO_3$) [5–8] have been proposed as candidate materials for resistive random access memorie (ReRAM). Various mechanisms have been suggested for resistance switching including carrier trapping/detrapping process [5], interface effects [3,6,7], metallic paths, and migration of oxygen ions [4,8]. In those mechanisms, defects play important roles since distribution and fundamental nature of defects strongly influence the electrical properties of materials, where disordered states are most likely to occur and have a random space and energy distributions. Since Anderson suggested the localization of carriers due to multiple scattering from the disordered defects [9], disordered states have been considered to induce weak localization (Anderson localization). Mott then reported that typical electrical conduction in disordered materials with weakly localized states followed the variable range hopping conduction model [10]. In a highly disordered or distorted state, electron–phonon interaction further increases the degree of localization. As a result, small polarons form and charge transport follows polaron conduction [11,12]. Small polaron formation in $SrTiO_3$ is typically accompanied by electron localization and has been investigated by far-infrared reflectively and luminescence studies [12–14]. In highly oxygen deficient Cr-doped $SrTiO_{3-\delta}$ thin films, small polarons formed and their conductivity was reduced due to strong electron–phonon interaction with the large polaron coupling constant $\alpha \sim 28$ [15]. This led to the suppression of resistance switching. However, the mechanism of electrical conduction in stoichiometric Cr-doped $SrTiO_3$ films is not yet clearly understood despite of the occurrence of resistance switching. This study reports in detail the electrical conduction and associated resistance switching mechanisms of stoichiometric Cr-doped $SrTiO_3$ films.

2. Experiments

A 60 nm-thick conducting oxide $La_{0.5}Sr_{0.5}CoO_3$ (LSCO) layer was deposited as a bottom electrode on a single crystalline (100) oriented $SrTiO_3$ substrate, followed by the deposition of a 60 nm thick 0.2% Cr-doped $SrTiO_3$ (Cr-STO_3) layer. The LSCO and Cr-STO_3 films were made by pulsed laser deposition (PLD). During deposition, the substrate was kept at 650 °C under an oxygen pressure of 10^{-1} Torr and then cooled under an oxygen pressure of 400 Torr. The 100 nm-thick Pt top electrodes were defined by a lift-off process using photolithography and sputtering. Current–voltage (I–V) measurements were carried out using a Keithley 2400 source meter and a low temperature probe station in the temperature

* Corresponding author. Tel.: +82 31 290 7397; fax: +82 31 290 7410.
E-mail address: jclee@skku.edu (J. Lee).

0038-1101/$ - see front matter © 2012 Elsevier Ltd. All rights reserved.
http://dx.doi.org/10.1016/j.sse.2012.05.007

range from 100 to 420 K. The voltage profile for the *I–V* measurement was 0 V → $-V_{max}$ → 0 V → $+V_{max}$ → 0 V. V_{max} was 10 V. The positive direction of the bias voltage corresponds to a positive bias applied to the Pt top electrode.

3. Results and discussion

Fig. 1 shows the *I–V* characteristics of the Pt/Cr-STO_3/LSCO structure in the voltage control mode at various temperatures. The initial (as-prepared) state was a high resistance state (HRS). The HRS was changed to a low resistance state (LRS) by applying a negative bias (0 → −10 V) to the Pt top electrode, whereas HRS was not changed by a positive bias (0 → 10 V). The resistance switching occurred without forming process often known to be necessary for the switching of several oxides. The LRS was progressively changed to the HRS only by a voltage sweep in the positive voltage region (0 → +10 V), which is essentially a bipolar character. The *I–V* characteristics did not change even after repeated stress cycles. The temperature dependence of *I–V* characteristics was investigated to clarify the leakage current mechanism. The *I–V* characteristics followed neither Schottky conduction nor Poole–Frenkel conduction. Therefore, the *I–V* characteristics were examined in terms of trap-controlled space-charge-limited conduction (SCLC) [16,17] and variable range hopping conduction (VRH) [10,18–20].

Fig. 2a presents the *I–V* characteristics of the negative sweep (0 → −10 V). The *I–V* characteristics of the HRS followed three distinct voltage regimes corresponding to three different slopes of the current. This leakage current behavior is well described by trap-controlled space-charge-limited conduction, in which Ohmic behavior at low voltages (0 → −1.2 V) is followed by trap-filled limit region (−1.2 V → −3 V) with $I \propto V^m$ dependence (m = 11–25) and trap-free space-charge-limited conduction (Child's law, $I \propto V^2$) above −3 V. A trap-filled limit voltage ($V_{TFL} = -1.2$ V) was obtained, which corresponds to the onset of a rapid increase in current (i.e., resistance switching to LRS) and is expressed as $V_{TFL} = 8qN_td^2/9K_\infty\varepsilon_0$ (d is the film thickness and N_t is the trap density) [17]. Using $K_\infty = n^2 = 5.76$ [21], N_t was estimated to be 1.2×10^{17} cm^{-3} at 200 K. The power law dependence of the current on the voltage in the trap-filled limit region indicates an exponential trap distribution ($I \propto V^m$, $m = l + 1$ with $l = T_t/T$, T_t is the characteristic temperature related to the trap distribution) [22], where the slope m typically decreases with temperature. The slope m obtained in the trap-filled limit region decreased with increasing the temperature from 100 K ($m \sim 25$) to 330 K ($m \sim 11$), indicating that the Cr-doped $SrTiO_3$ films has localized states with an exponential trap distribution.

It is expected that the localized state close to conduction band edge (i.e., shallow trap) is heavily populated and its density decreases exponentially away from the conduction band edge. Injected

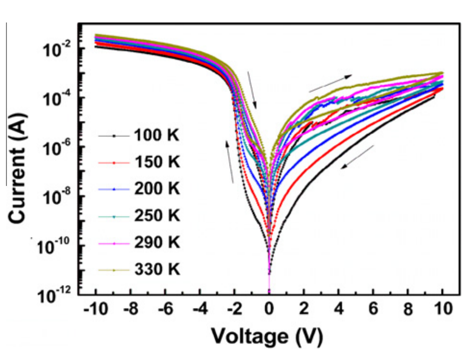

Fig. 1. Current vs. voltage (*I–V*) hysteretic curve of the Pt/Cr-STO/LSCO structure at various temperatures.

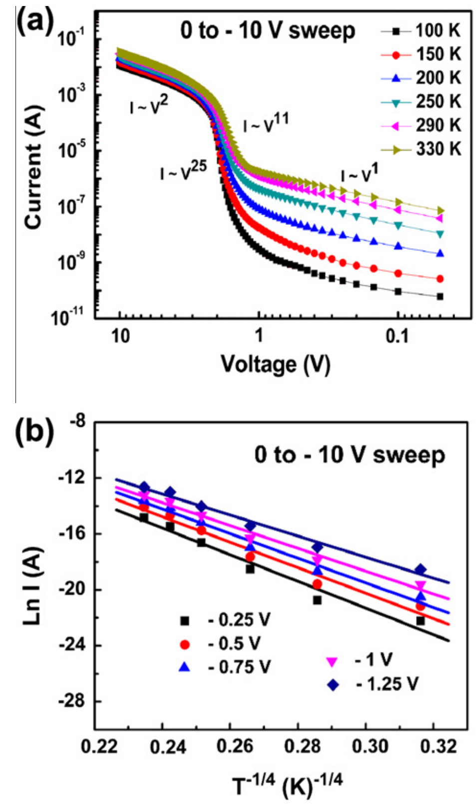

Fig. 2. (a) Current vs. voltage characteristic at various temperatures and (b) temperature dependence of current in a sweep from 0 to −10 V.

carriers would then influence the filling of the localized states through quasi-Fermi level positioning and further conducting (or resistance) state. *I–V* characteristics were examined in the low negative voltage region (0 → −2 V) to find whether the carrier injection affects states' occupancies. Fig. 2b shows the linear dependence of ln(I) vs. ($T^{-1/4}$) below −1.25 V that suggests VRH conduction, typical of disordered materials and expressed by the following equation:

$$I(T) \propto \exp[-(T_0/T)^{1/4}], \quad (1)$$

where $T_0 = C_T \frac{\alpha^3}{k_B N(E_F)}$, $C_T = 24/\pi$, α is the inverse length on which the amplitude of the wave function falls down, k_B is the Boltzmann constant, T_0 is an indirect measurement of the density of localized states participating in hopping conduction and $N(E_F)$ is the energy density of localized sites at the quasi-Fermi level. For VRH conduction, a material requires many empty sites for hopping. The available hopping carrier density inside the film and the injected carrier density are not sufficient to fill the empty trap sites fully. Therefore, conduction behavior follows trap-controlled SCL conduction as well as VRH conduction. However, at $V_{TFL} = -1.2$ V, all the empty sites are filled by injected carriers and available hopping carriers, leading to the rapid increase of current with increasing the negative voltage, as shown in Fig. 2a. Accordingly, the conduction mechanism changes from VRH conduction to trap-filled limit conduction and resistance switches from HRS to LRS. At further increase in the negative bias voltage above −3 V, the current followed a square law with its temperature independence, characteristic of Child's law.

The hopping carrier density $N_{hopping}$ was estimated at the threshold voltage in VRH conduction, $V_{TFL} = -1.2$ V in order to understand the transition from VRH to trap-filled limit conduction. $N(E_F)$ estimated from the temperature dependence of VRH conduction was